

## Thermoelectric properties of Ca-doped $\gamma$ - $\text{Na}_x\text{CoO}_2$

Yasuhiro Ono, Nobuhiko Kato, Yuzuru Miyazaki  
and Tsuyoshi Kajitani

Department of Applied Physics, Graduate School of Engineering, Tohoku University, Sendai, 980-8579, Japan

Fax: 81-22-217-7982, e-mail:ono@crystal.apph.tohoku.ac.jp

Single-phase polycrystalline samples of  $\gamma\text{-Na}_{0.70}\text{Ca}_x\text{CoO}_{2-\delta}$  are successfully synthesized in the concentration range,  $0 \leq x \leq 0.07$ , by a two-step sintering procedure, i.e.,  $\gamma\text{-Na}_{0.70}\text{CoO}_{2-\delta}$  powder mixed with an appropriate amount of  $\text{Ca}(\text{NO}_3)_2 \cdot 4\text{H}_2\text{O}$  is sintered at 873 K and 1123 K in air for 12 h. ICP analysis data indicate that Na content ( $\text{Na}/\text{Co} = 0.64\text{--}0.67$ ) is slightly lower than the nominal one (0.70). Oxygen deficiency is determined by the automated iodometric titration technique ( $\delta = 0.025\text{--}0.033$ ). In this system, formal valence of Co ion linearly decreases from +3.27(2) at  $x=0$  to +3.16(2) at  $x=0.07$ , implying electron doping. We have studied thermoelectric properties of  $\gamma\text{-Na}_{0.70}\text{Ca}_x\text{CoO}_{2-\delta}$  at high temperature. Both electrical resistivity,  $\rho$ , and Seebeck coefficient,  $S$ , almost linearly increase with increasing temperature. The maximum power factor,  $S^2/\rho = 6.4 \times 10^{-4} \text{ W m}^{-1}\text{K}^{-2}$  at 985 K, is obtained for the sample with  $x=0.0175$ . Thermal conductivity of the  $x=0.07$  sample is 7–10% lower than that of  $\gamma\text{-Na}_{0.70}\text{CoO}_{2-\delta}$  ( $x=0$ ).

Key words: thermoelectric material, layered oxide,  $\gamma\text{-Na}_x\text{CoO}_{2-\delta}$ , Ca-doping

### 1. INTRODUCTION

Recent discovery of potential oxide thermoelectric (TE) materials has attracted much attention, since high temperature applications such as power generation utilizing waste heat from factories and engines can be expected for these materials [1–4]. The layered cobaltite,  $\gamma\text{-Na}_x\text{CoO}_{2-\delta}$ , is one of the most promising p-type TE materials and exhibits high Seebeck coefficient ( $S=200 \mu\text{V K}^{-1}$ ), low electrical resistivity ( $\rho=5.2 \mu\Omega \text{ m}$ ) and low thermal conductivity ( $\kappa=5.1 \text{ W m}^{-1}\text{K}^{-1}$ ) at  $T=800 \text{ K}$  [5]. The dimensionless figure of merit,  $ZT=S^2T/\rho\kappa$ , for a single crystal of  $\gamma\text{-Na}_x\text{CoO}_{2-\delta}$  becomes 1.2 at this temperature, which satisfies the empirical criterion for practical applications ( $ZT \geq 1$ ). Despite of high carrier density ( $10^{27}\text{--}10^{28} \text{ m}^{-3}$ ), the Seebeck coefficient of  $\gamma\text{-Na}_x\text{CoO}_{2-\delta}$  is unusually high. It is difficult to understand such high Seebeck coefficient within the framework of a conventional band picture.

The substitution effects of Li, Ag, Mg, Ca, Sr, Ba and La for Na in polycrystalline  $\gamma\text{-Na}_x\text{CoO}_{2-\delta}$  have been systematically studied by Yakabe et al. [6], Fujita et al.

[7], Kawata et al. [8] and Ishikawa et al [9]. Kawata et al. [8] reported that the Seebeck coefficient,  $S$ , appreciably increases with increasing  $x$  in  $\gamma\text{-Na}_{0.55-x}\text{Ca}_x\text{CoO}_2$ . Unfortunately, the electrical resistivity,  $\rho$ , was so high that the TE performance was not improved markedly [8]. Recently, we found that Ca can be introduced into the highly vacant Na sheet of  $\gamma\text{-Na}_x\text{CoO}_{2-\delta}$  without changing Na content remarkably ( $\text{Na}/\text{Co}=0.63\text{--}0.67$ ). In this paper, synthesis, chemical analyses and thermoelectric properties of  $\gamma\text{-Na}_{0.70}\text{Ca}_x\text{CoO}_{2-\delta}$  are presented.

### 2. EXPERIMENTAL

Polycrystalline samples of  $\gamma\text{-Na}_{0.70}\text{CoO}_{2-\delta}$  were prepared from  $\text{Na}_2\text{CO}_3$  (99.5%) and  $\text{Co}_3\text{O}_4$  (99.9%) by a conventional solid-state reaction as described in the previous report [10]. The Ca-doped polycrystalline samples,  $\gamma\text{-Na}_{0.70}\text{Ca}_x\text{CoO}_{2-\delta}$  ( $x=0.0175, 0.035, 0.07, 0.105$  and  $0.175$ ), were prepared by the following two-step sintering procedure. The starting materials,  $\gamma\text{-Na}_{0.70}\text{CoO}_{2-\delta}$  and  $\text{Ca}(\text{NO}_3)_2 \cdot 4\text{H}_2\text{O}$  (99.9%), were

thoroughly mixed, sintered at 873 K for 12 h in air and subsequently homogenized at 1123 K for 12 h in air with an intermediate grinding. Powder X-ray diffraction intensities of these samples were measured using a RIGAKU RAD-X diffractometer ( $\text{CuK}\alpha$ ) equipped with a curved-graphite monochromator, which is needed to remove fluorescent X-ray of Co ion. Na, Ca and Co contents in the samples were determined by the inductively coupled plasma (ICP) analysis. The valence of Co ion and the oxygen deficiency were evaluated by a standard iodometric titration technique using an auto buret AUT-501 (TOA DKK), which was operated in Ar atmosphere to avoid the oxidation of Co ion. The electrical resistivity and the Seebeck coefficient were measured in the temperature range from 480 K to 985 K using an automated Seebeck coefficient measuring apparatus, Ozawa RZ2001i. The thermal conductivity measurement was performed using a steady-state heat-flux measuring apparatus, ULVAC GH-1S.

### 3. RESULTS AND DISCUSSION

#### 3.1 Powder X-ray diffraction

Figure 1 shows the observed powder X-ray diffraction patterns. A few impurity peaks marked by closed circles were observed for the samples with  $x=0.105$  and  $0.175$ . The second phase in these heavily

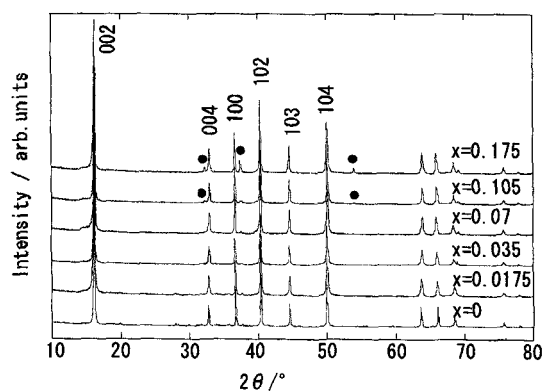


Fig.1. Powder X-ray diffraction patterns of  $\gamma\text{-Na}_{0.70}\text{Ca}_x\text{CoO}_{2-\delta}$ . Closed circles indicate the impurity peaks (CaO).

Ca-doped samples was identified as CaO. Except for those impurity peaks, the diffraction patterns of the Ca-doped samples are almost the same as that of

$\gamma\text{-Na}_{0.70}\text{CoO}_{2-\delta}$  ( $x=0$ ). There are many vacant sites in  $\text{Na}^+$  layer of  $\gamma\text{-Na}_{0.70}\text{CoO}_{2-\delta}$  [10] and it is likely to introduce other ions to these sites. Since the ionic radius of  $\text{Ca}^{2+}$  (0.100 nm) is similar to that of  $\text{Na}^+$  (0.102 nm) [11], the doped  $\text{Ca}^{2+}$  can easily occupy the vacant  $\text{Na}^+$  site. Lattice parameters of the present samples were determined by the least-squares calculation from the diffraction angles,  $2\theta$ , of well-defined Bragg reflections. Figure 2 shows the lattice parameters,  $a$  and  $c$ , as a function of Ca content, where their error-bars are inside the symbols. In  $0 \leq x \leq 0.07$ , the lattice parameter,  $a$ , slightly increases with increasing  $x$ , while the lattice

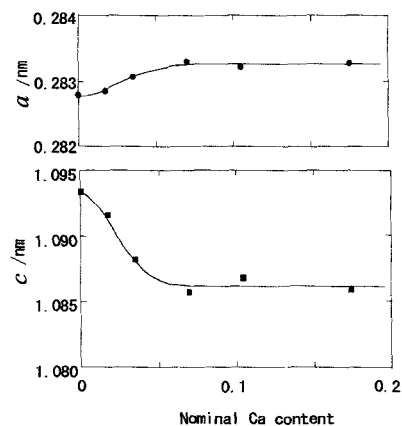


Fig.2. Lattice parameters ( $a$  and  $c$ ) vs. nominal Ca content in  $\gamma\text{-Na}_{0.70}\text{Ca}_x\text{CoO}_{2-\delta}$  system.

parameter,  $c$ , shows relatively large decrease. Above  $x=0.07$ , both  $a$  and  $c$  remain almost constant. X-ray diffraction analysis indicates that the single-phase  $\gamma\text{-Na}_{0.70}\text{Ca}_x\text{CoO}_{2-\delta}$  is successfully synthesized in the range,  $0 \leq x \leq 0.07$ .

#### 3.2 Chemical analysis

The nominal and analyzed chemical compositions of the present samples are listed in Table 1. The analyzed Na content (0.63–0.67) is slightly lower than the nominal one (0.70) due to the evaporation of Na during the sintering [12]. On the other hand, there are good agreements between the nominal and analyzed Ca contents. The oxygen deficiency determined by the titration measurement is negligibly small ( $\delta=0.025$ – $0.033$ ) in the single-phase region. Figure 3 shows the valence of Co ion versus Ca content,  $x$ . In the single-phase region, the valence of Co ion linearly

decreases from +3.27(2) at  $x=0$  to +3.16(2) at  $x=0.07$ , implying electron doping. These fractional values are due to the coexistence of  $\text{Co}^{3+}$  and  $\text{Co}^{4+}$  [10,13], i.e., the mixed valence state of Co ions.

Table I. Chemical compositions of  $\gamma\text{-Na}_{0.70}\text{Ca}_x\text{CoO}_{2-\delta}$ .

$x$	Na	Ca	Co	$\delta$
0	0.67	0	1	0.031±0.003
0.0175	0.66	0.02	1	0.033±0.002
0.035	0.65	0.04	1	0.028±0.004
0.070	0.64	0.08	1	0.025±0.002
0.105	0.63	0.11	1	-0.005±0.003
0.175	0.63	0.16	1	—

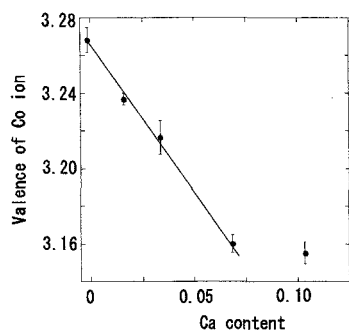


Fig.3. Valence of Co ion vs. nominal Ca content in  $\gamma\text{-Na}_{0.70}\text{Ca}_x\text{CoO}_{2-\delta}$  system.

### 3.3 Thermoelectric properties

Figures 4(a) and (b) show temperature variations of the electrical resistivity,  $\rho$ , and the Seebeck coefficient,  $S$ , respectively. Linear  $\rho$ - $T$  curves in Fig.4(a) represent metallic conduction in the measured temperature range. Both  $\rho$  and  $S$  tend to increase with increasing Ca content,  $x$ . The major carriers in  $\gamma\text{-Na}_x\text{CoO}_{2-\delta}$  ( $x=0$ ) are the electron holes and the population of holes decreases with increasing  $x$ . Accordingly, the increase in  $\rho$  and  $S$  is due to the decrease of holes. One may notice that the  $\rho$  values of the  $x=0.0175$  sample are nearly equal to those of  $\gamma\text{-Na}_{0.70}\text{CoO}_{2-\delta}$ . It is known that the  $\rho$  value of polycrystalline  $\gamma\text{-Na}_x\text{CoO}_{2-\delta}$  is strongly affected by the grain size [14] and the grain orientation [15]. Thus, the lowering of  $\rho$  in the  $x=0.0175$  sample is possibly related with the morphology. The  $S$  values of this sample ( $x=0.0175$ ) are almost at the same level as those of the  $x=0.035$  sample, though the effect of grain size on  $S$  was not observed in the polycrystalline  $\gamma\text{-Na}_x\text{CoO}_{2-\delta}$  [15].

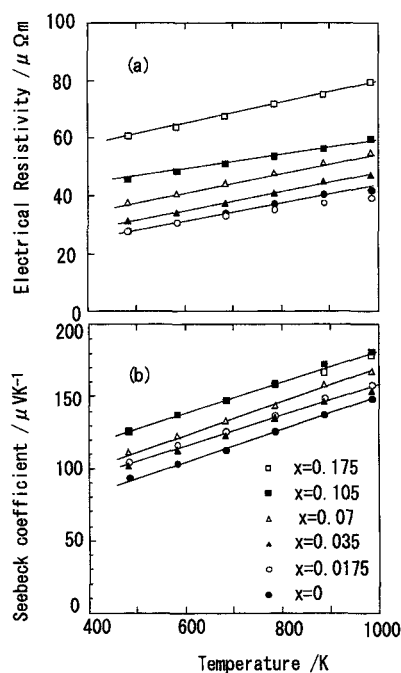


Fig.4. Temperature variations of electrical resistivity (a) and Seebeck coefficient (b) of  $\gamma\text{-Na}_{0.70}\text{Ca}_x\text{CoO}_{2-\delta}$ .

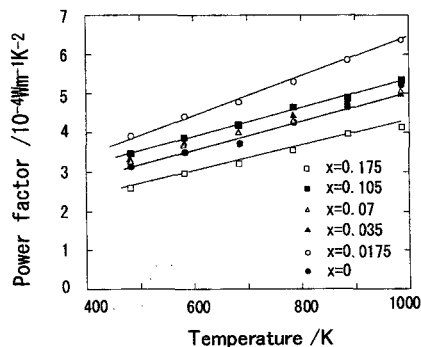


Fig.5. Temperature variation of power factor of  $\gamma\text{-Na}_{0.70}\text{Ca}_x\text{CoO}_{2-\delta}$ .

Figure 5 shows temperature variation of power factor,  $S^2/\rho$ . The maximum power factor,  $6.4 \times 10^{-4} \text{ W m}^{-1} \text{ K}^{-2}$  at 985 K, is obtained at  $x=0.0175$ . This value is about 1.3 times larger than that of the end member  $\gamma\text{-Na}_{0.70}\text{CoO}_{2-\delta}$  ( $x=0$ ) in the present results.

Figure 6 shows temperature variation of thermal conductivity,  $\kappa$ .  $\gamma\text{-Na}_x\text{CoO}_{2-\delta}$  ( $x=0$ ) and the 0.07 sample exhibit similar temperature dependence of  $\kappa$ . The  $\kappa$  values of the  $x=0.07$  sample are 7–10% lower than those of  $\gamma\text{-Na}_{0.70}\text{CoO}_{2-\delta}$  ( $x=0$ ). The thermal conductivity of the  $x=0.035$  sample monotonically increases with increasing temperature. The dimensionless figure of merit,  $ZT=S^2T/\rho\kappa$ , was thus

estimated to be 0.12, 0.14 and 0.15 for the present samples,  $\gamma$ - $\text{Na}_{0.70}\text{Ca}_x\text{CoO}_{2.6}$  with  $x=0$ , 0.035 and 0.07 at 580 K, respectively.

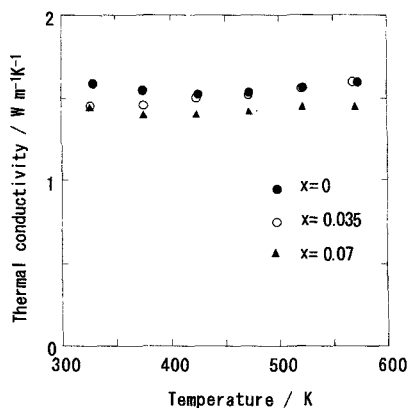


Fig.6 Temperature variation of thermal conductivity of  $\gamma$ - $\text{Na}_{0.70}\text{Ca}_x\text{CoO}_{2.6}$  ( $x=0$ , 0.035 and 0.07).

#### 4. CONCLUSION

The single-phase polycrystalline samples of  $\gamma$ - $\text{Na}_{0.70}\text{Ca}_x\text{CoO}_{2.6}$  with the negligibly small oxygen deficiency ( $\delta=0.025$ – $0.033$ ) were successfully synthesized in the range,  $0 \leq x \leq 0.07$ . The valence of Co ion linearly decreases from +3.27(2) at  $x=0$  to +3.16(2) at  $x=0.07$ . All samples are metallic in the temperature range from 480 K to 985 K. The maximum power factor was obtained at  $x=0.0175$  because the enhancement of Seebeck coefficient and the reduction in electrical resistivity occur simultaneously at  $x=0.0175$ . The thermal conductivity of the  $x=0.07$  sample is 7–10% lower than that of  $\gamma$ - $\text{Na}_{0.70}\text{CoO}_{2.6}$  ( $x=0$ ). The Ca-doping is an effective method to improve the TE performance of  $\gamma$ - $\text{Na}_{0.70}\text{CoO}_{2.6}$ .

**ACKNOWLEDGEMENT** This research was partly supported by CREST (Core Research for Evolution Science and Technology) project of JST (Japan Science and Technology Corporation).

#### References

- [1] I.Terasaki, Y.Sasago and K.Uchinokura, *Phys.Rev.*, **B56**, R12685-R12687 (1997).
- [2] M.Yasukawa and N.Murayama, *Mater.Sci.Eng.*, **B54**, 64-69. (1998).
- [3] R.Funahashi, I.Matsubara and S.Sodeoka, *Appl.Phys.Lett.*, **76**, 2385-2387 (2000).
- [4] Y.Miyazaki, K.Kudo, M.Akoshima, Y.Ono, Y.Koike and T.Kajitani, *Jpn.J.Appl.Phys.*, **40**, L531-L534 (2001).
- [5] K.Fujita, T.Mochida and K.Nakamura, *Jpn.J.Appl.Phys.*, **40** 4644-4647 (2001).
- [6] H.Yakabe, K.Fujita, K.Nakamura and K.Kikuchi, *Proc.17<sup>th</sup> International Conference on Thermoelectricals*, pp.551-558 (1998).
- [7] K.Fujita, K.Nakamura and S.Yamashita, *Proc.18<sup>th</sup> International Conference on Thermoelectricals*, pp.481-484 (1999).
- [8] T.Kawata, Y.Iguchi, T.Itoh, K.Takahata and I.Terasaki, *Phys.Rev.*, **B60**, 10584-10587(1999).
- [9] R.Ishikawa, Y.Ono, Y.Miyazaki and T.Kajitani, *Jpn.J.Appl.Phys.*, **41**, L337-L339(2002).
- [10] Y.Ono, R.Ishikawa, Y.Miyazaki and T.Kajitani, *J.Phys.Soc.Jpn.*, **70**, Suppl.A, 235-238(2000).
- [11] R.D.Shannon and C.T.Prewitt, *Acta Cryst.*, **B25**, 925-946(1969).
- [12] T.Motohashi, E.Naujalis, R.Ueda, K.Isawa, M.Karppinen and H.Yamauchi, *Appl.Phys.Lett.*, **79**, 1480-1482(2001).
- [13] R.Ray, A.Ghoshray, K.Ghoshray and S.Nakamura, *Phys.Rev.*, **B59**, 9454-9461(1999).
- [14] K.Fujita, K.Nakamura and H.Yakabe, "Thermoelectrical Oxide", Ed. By K.Koumoto, I.Terasaki and N.Murayama, Trivandrum (2002) pp.21-44.
- [15] S.Tajima, T.Tani, S.Isobe and K.Koumoto, *Mater. Sci.Eng.*, **B86**, 20-25(2001).

(Received October 13, 2003; Accepted January 16, 2004)